OXFORD

ORIGINAL ARTICLE

Pathway-Specific Genetic Risk for Alzheimer's Disease Differentiates Regional Patterns of Cortical Atrophy in Older Adults

Svenja Caspers[1,2,3,*], Melanie E. Röckner[1,4,*], Christiane Jockwitz[1,3,5], Nora Bittner[1,2], Alexander Teumer[6], Stefan Herms[7,4,8], Per Hoffmann[1,7,4,8], Markus M. Nöthen[4,8], Susanne Moebus[9], Katrin Amunts[1,3,10], Sven Cichon[1,7,11,4,8,*] and Thomas W. Mühleisen[1,7,10,*]

[1]Institute of Neuroscience and Medicine (INM-1), Research Centre Jülich, D-52428 Jülich, Germany, [2]Institute for Anatomy I, Medical Faculty, Heinrich Heine University Düsseldorf, D-40225 Düsseldorf, Germany, [3]JARA-BRAIN, Jülich-Aachen Research Alliance, D-52428 Jülich, Germany, [4]Institute of Human Genetics, University Hospital Bonn, D-53127 Bonn, Germany, [5]Department of Psychiatry, Psychotherapy and Psychosomatics, RWTH Aachen University, Medical Faculty, D-52074 Aachen, Germany, [6]Institute for Community Medicine, University Medicine Greifswald, D-17475 Greifswald, Germany, [7]Department of Biomedicine, University of Basel, CH-4031 Basel, Switzerland, [8]Department of Genomics, Life & Brain Center, University of Bonn, D-53127 Bonn, Germany, [9]Institute for Medical Informatics, Biometry and Epidemiology, University of Duisburg-Essen, D-45122 Essen, Germany, [10]C. & O. Vogt Institute for Brain Research, Heinrich Heine University Düsseldorf, D-40225 Düsseldorf, Germany and [11]Institute of Medical Genetics and Pathology, University Hospital Basel, CH-4031 Basel, Switzerland

Address correspondence to Sven Cichon, Institute of Neuroscience and Medicine (INM-1), Research Centre Jülich, Leo-Brandt-Strasse, D-52428 Jülich, Germany. Email: s.cichon@fz-juelich.de

*Svenja Caspers, Melanie E. Röckner, Sven Cichon, and Thomas W. Mühleisen contributed equally to this work

Abstract

Brain aging is highly variable and represents a challenge to delimit aging from disease processes. Moreover, genetic factors may influence both aging and disease. Here we focused on this issue and investigated effects of multiple genetic loci previously identified to be associated with late-onset Alzheimer's disease (AD) on brain structure of older adults from a population sample. We calculated a genetic risk score (GRS) using genome-wide significant single-nucleotide polymorphisms from genome-wide association studies of AD and tested its effect on cortical thickness (CT). We observed a common pattern of cortical thinning (right inferior frontal, left posterior temporal, medial occipital cortex). To identify CT changes by specific biological processes, we subdivided the GRS effect according to AD-associated pathways and performed follow-up analyses. The common pattern from the main analysis was further differentiated by pathway-specific effects yielding a more bilateral pattern. Further findings were located in the superior parietal and mid/anterior cingulate regions representing 2 unique pathway-specific patterns. All patterns, except the superior parietal pattern, were influenced by

apolipoprotein E. Our step-wise approach revealed atrophy patterns that partially resembled imaging findings in early stages of AD. Our study provides evidence that genetic burden for AD contributes to structural brain variability in normal aging.

Key words: aging, Alzheimer's disease, atrophy, cortical thickness, genetic risk score, SNP

Introduction

Aging of the brain is accompanied by a decline of cognitive functions, the reorganization of functional networks, and structural atrophy (Reuter-Lorenz and Lustig 2005; Goh and Park 2009; Park and Reuter-Lorenz 2009; Reuter-Lorenz and Park 2014). The degree of such changes, however, is highly variable between individuals and there is a continuous transition from normal variability into clinically relevant states of disease (Pini et al. 2016). Late-onset Alzheimer's disease (AD) is an increasingly prevalent neurodegenerative disease that is associated with gray matter (GM) atrophy (Karlawish et al. 2017). Since neurodegenerative and aging processes are influenced by genetic and environmental factors, one may speculate to what extent these factors contribute to brain variability observed in normal aging.

The apolipoprotein E gene (*APOE*) has been identified as the first susceptibility locus for AD (Saunders et al. 1993, Strittmatter et al. 1993). Genome-wide association studies (GWAS) have later explored additional loci of AD (Sims and Williams 2016). Since we aimed to focus on loci that show the highest probability of being associated with AD, we preferred single-nucleotide polymorphisms (SNPs) that provide genome-wide significance and evidence for replication. In doing so, we selected SNPs from GWAS of AD at 20 loci that harbor genes with functions in 7 biological pathways (Guerreiro et al. 2013; Rosenthal and Kamboh 2014; Karch and Goate 2015; Van Cauwenberghe et al. 2016; Table 1). The pathway cholesterol metabolism contains 4 AD associated gene loci (*APOE, ABCA7, CLU, SLC24A4-RIN3*) from which *APOE* plays a role in cholesterol transport, neural plasticity, and inflammation. Apolipoprotein precursor (APP) metabolism shares 3 AD genes with cholesterol metabolism (*APOE, ABCA7, CLU*), while 3 AD genes are different (*INPP5D, PICALM, SORL1*). Microtubule-associated protein tau (MAPT) metabolism comprises 3 AD genes (*BIN1, CASS4, FERMT2*) and plays a key role in tau pathology. *CASS4* and *FERMT2* add up with 2 other AD genes (*CELF1, NME8*) in the cytoskeleton/axon development pathway. The immune response pathway harbors 8 AD gene loci (*ABCA7, CLU, CR1, EPHA1, HLA-DRB5-DRB1, INPP5D, MEF2C, MS4A6A*) of which *CR1, HLA-DRB5-DRB1*, and *MS4A6A* do not overlap with the other pathways. APP trafficking and amyloid β clearance via clathrin-mediated endocytosis is a pathway that integrates 8 AD gene loci (*BIN1, CD2AP, EPHA1, MEF2C, PICALM, PTK2B, SLC24A4-RIN3, SORL1*) in which *CD2AP* and *PTK2B* occur only here and *BIN1* is shared with MAPT metabolism. Epigenetics is the only pathway that includes a single gene (*ZCWPW1*). Overall, the majority of AD genes contribute to 2 or more pathways suggesting that specific gene functions are linked in AD pathogenesis.

Several studies have used a genetic risk score (GRS) approach to characterize effects of these loci in parallel and found associations with cognitive decline, hippocampal volume loss in young individuals, and in population life-span cohorts as well as in patients with mild cognitive impairment (MCI) or dementia, for whom also a relation to AD pathology and clinical progression has been demonstrated (Martiskainen et al. 2015; Habes et al. 2016; Harrison et al. 2016; Louwersheimer et al. 2016; Lupton et al. 2016; Mormino et al. 2016). However, another study has found no association between a GRS for AD risk and cognition in a large group of older subjects (Harris et al. 2014).

It has been demonstrated that cortical thickness (CT) is a heritable and sensitive biomarker to investigate the effects of aging on brain structure (Winkler et al. 2010; Sabuncu et al. 2011; Hwang et al. 2016). In fact, reduced CT in healthy older adults (Sabuncu et al. 2012) and reduced hippocampal volume in healthy young subjects with higher AD-GRS, even after exclusion of *APOE* from the risk score has been reported (Foley et al. 2017). Moreover, *APOE* seemed to have a more pronounced influence on cognitive function in the general population than other AD-associated risk genes (Verhaaren et al. 2013) and cognition and beta-amyloid deposition in a large sample of older adults with increased risk for AD (Darst et al. 2016). These findings suggest that susceptibility genes for AD may have differential effects on cognition and brain structure in normal aging and that *APOE* plays a strong role in these processes.

In the present study, we aimed to extend this knowledge by investigating developing patterns of cortical atrophy (CT) in normal aging attributable to different loads of risk for AD (overall and pathway-specific analyses) using older adults from a large population-based cohort from Germany (1000BRAINS).

Materials and Methods

Sample Data

The study sample consisted of older adults from the general population in Western Germany (Bochum, Essen, Mülheim a. d. Ruhr). The sample was drawn from 1000BRAINS, an epidemiological cohort investigating influences of interindividual variability of brain structure, function, and connectivity at higher age (Caspers et al. 2014), based on the Heinz Nixdorf Recall study (Schmermund et al. 2002). Written informed consent was obtained from all individuals before participation. Protocols and procedures were approved by the Ethics Committee of the Essen University Hospital, Germany.

Since 1000BRAINS follows a population design, no a priori exclusion criteria were applied on the study sample. Participants were screened for symptoms of dementia (score < 9) or MCI (9 ≤ score < 12) using the DemTect Test (Kalbe et al. 2004). German ancestry was assigned to participants based on self-reported ancestry, with possible population stratification being checked by a SNP-based principal component analysis. Of 558 participants, 14 were excluded due to the following reasons: stroke ($n = 2$), failed magnetic resonance (MR) image processing ($n = 5$), genetic quality control and imputation ($n = 7$), resulting in a final sample of 544 individuals with mean age of 67.3 years. An overview of the major demographic variables of the study sample is provided by Table 2.

Genetic Data

Extraction of DNA, Microarray Genotyping, and Computational Imputation of SNPs

Lymphocyte DNA from participants was isolated from ethylene-diaminetetraacetic acid-coagulated venous blood by a Chemagic

Table 1 Composition of the GRS total

Chr	Gene	SNP	MA	OR	Cholesterol metabolism	APP metabolism	MAPT metabolism	Cytoskeleton, axon development	Immune response	Endocytosis	Epigenetics
19q13.32	**TOMM40/APOE**	rs2075650	G	2.53	■	■				■	
2q14.3	BIN1	rs6733839	T	1.22			■			■	
1q32.2	CR1	rs6656401	A	1.18					■	■	
19p13.3	ABCA7	rs4147929	A	1.15	■	■			■	■	
14q22.1	FERMT2	rs17125944	C	1.14			■	■	■		
6p21.32	HLA-DRB5, HLA-DRB1	rs9271192	C	1.11					■		
8p21.2	PTK2B	rs28834970	C	1.10						■	
6p12.3	CD2AP	rs10948363	G	1.10						■	
2q37.1	INPP5D	rs35349669	T	1.08		■			■		
11p11.2	CELF1	rs10838725	C	1.08				■			
5q14.3	MEF2C	rs190982	G	0.93					■		
7p14.1	NME8	rs2718058	G	0.93				■			
7q22.1	ZCWPW1	rs1476679	C	0.91							
14q32.12	SLC24A4, RIN3	rs10498633	T	0.91	■	■				■	
11q12.2	MS4A6A	rs983392	G	0.90						■	
7q35	EPHA1	rs11771145	A	0.90							■
20q13.31	CASS4	rs7274581	C	0.88			■	■			
11q14.2	PICALM	rs10792832	A	0.87		■				■	
8p21.1	CLU	rs9331896	C	0.86	■	■			■		
11q24.1	SORL1	rs11218343	C	0.77		■				■	

Genes were sorted according to effects from SNPs (vertical) and pathways were sorted according to effects from pathway-specific GRS (horizontal). APP, amyloid β precursor protein; MA, minor allele in controls of European ancestry; MAPT, microtubuli-associated protein tau; OR, odds ratios (SNP effects) refer to minor alleles according to Lambert et al. (2013).

Table 2 Demographic data of the study sample from 1000BRAINS

Participants (n = 544)	
Age (mean ± SD)	67.3 ± 6.7
Gender (male/female)	298/246
APOE ε4 carriers (rs2075650-G)	
risk alleles/non-risk alleles (GG + GA/AA)	150/394

Magnetic Separation Module I (Perkin-Elmer, Rodgau, Germany). DNA samples were genome-wide genotyped using Infinium assays (Illumina, San Diego, CA, USA) for the microarrays HumanOmniExpress (n = 391), HumanOmni1-Quad (n = 115), and HumanCoreExome (n = 52). Quality control of raw genotype data comprised an exclusion of SNPs (deviation from Hardy–Weinberg equilibrium: $P \leq 1 \times 10^{-4}$; genotyping call rate: cr ≤ 95%; minor allele frequency: MAF ≤ 3%) and participants (SNP-based principal component analysis: > 8 s.d. of the mean in 1 of the first 10 principal components; mismatch between self-reported and X-chromosomal-derived sex). To increase the number of available SNPs and decrease the number of missing genotype calls, dosage data were generated for all participants using IMPUTE (version 2.3.1) as tool and phased haplotypes from The 1000 Genomes Project (ALL macGT1 reference panel, phase 1, release 3, March 2012) as reference. Genetic data were imputed for each microarray type separately and combined afterwards. A multidimensional scaling of the combined data was performed which showed no indication of array-specific batch effects (Supplementary Fig. S1).

Selection of SNPs, Genes, and Pathways Associated with Alzheimer's Disease

Selection of candidate SNPs based on designs and results from GWAS of the International Genomics of Alzheimer's Project (Harold et al. 2009; Lambert et al. 2013) and the Alzheimer's Disease Neuroimaging Initiative (Sabuncu et al. 2012), and other groups (Chauhan et al. 2015). SNPs were extracted from genome-wide imputed data of participants using the most likely genotypes that were generated by an R software package (R Development Core Team 2010). The resulting 20 genome-wide significant, linkage disequilibrium-independent SNPs ($P < 5 \times 10^{-8}$; $r^2 < 0.8$) were mapped to the nearest genes (RefSeq definitions, GRCh37/hg19 genome assembly). For the construction of GRS, we used a two-tiered strategy: we first constructed a "total" GRS including all 20 selected SNPs, a commonly used strategy to perform GRS analyses. This strategy does not include biological information and may include a mixture of SNPs acting in different or even opposite directions at a biological level. In order to address this point and disentangle the action of different biological pathways, we aimed at grouping the GRS-SNPs into different biological processes and build "pathway-specific" GRS. For this step, all SNPs had to be linked to genes through linkage disequilibrium (LD) with SNPs located in these genes. These genes were subsequently annotated to biological pathways according to definitions reported by Karch and Goate (2015) and Guerreiro et al. (2013), resulting in 7 pathways of interest (Table 1).

Most of the GRS-SNPs tag variation within AD-associated genes. However, 4 GRS-SNPs may be considered as "intergenic" since they are not directly mapping to a gene. Knowledge about expressed quantitative trait loci (eQTLs) shows that they tag variation in regions regulating expression of genes in cis.

The GWAS SNP rs6733839 is located on chromosome 2q14.3 between genes *BIN1* and *CYP27C1*. In particular, rs6733839 points to a small region (LD block) where a neighboring marker (rs59335482) increases *BIN1* expression in the frontal cortex (Chapuis et al. 2013). Analysis of cell type-specific expression showed that *BIN1* is most highly expressed in microglia (Karch et al. 2016). Functional studies in *Drosophila* and human neuroblastoma cells suggest that *BIN1* mediates AD risk by modulating Tau pathology (Chapuis et al. 2013).

SNP rs2718058 (7p14.1) is located at the GWAS locus *GPR141-NME8*. In the brain, rs2718058 drives expression of *GPR141* in the frontal cortex and putamen (Karch et al. 2016). *GPR141* encodes an orphan receptor of the Class A rhodopsin-like G protein-coupled receptors; an important paralog is *GPR174* that encodes a putative receptor for purine ligands (www.genecards.org).

SNP rs9271192 (6p21.32) tags a larger cluster of 5 genes (*MS4A3, MS4A2, MS4A6A, MS4A4A, MS4A6E*) from the human leukocyte antigen (HLA) system. The risk allele of rs9271192 significantly associated with *HLA-DRB1* expression in both temporal cortex and cerebellum in patients with AD (Allen et al. 2015); *HLA-DRB1* is 1 of the 2 genes closest to the SNP. As *BIN1*, *HLA-DRB1* shows the highest expression in microglia (Karch et al. 2016).

SNP rs10792832 (11q14.2) is located at the *PICALM-EED* locus. In the brain, rs10792832 influences *EED* expression in putamen, thalamus, and medulla (Karch et al. 2016). Moreover, *EED* expression is neuron-specific in brains of AD patients (Karch et al. 2016). *EED* encodes a transcriptional repressor of the Polycomb-group family (www.genecards.org).

MRI data

Image Acquisition

High-resolution T1-weighted MRIs were acquired on a 3 Tesla Magnetom Tim-Trio scanner (Siemens, Erlangen, Germany) using a 32-channel head coil (176 slices, slice thickness 1 mm, repetition time [TR] = 2250 ms, echo time [TE] 3.03 ms, field of view [FoV] = 256 × 256 mm, flip angle = 9°, voxel resolution 1 × 1 × 1 mm), as part of the MRI protocol from 1000BRAINS (Caspers et al. 2014).

Image Processing and Computation of CT

T1-weighted structural MRI were preprocessed using the automated pipeline for surface reconstruction implemented in the FreeSurfer Software package (version 5.3.0; Dale et al. 1999; Fischl et al. 1999; Fischl and Dale 2000; http://surfer.nmr.mgh.harvard.edu). Before entering the FreeSurfer pipeline, MRI data were segmented into GM, white matter (WM), and cerebrospinal fluid using the unified segmentation approach (Ashburner and Friston 2005) implemented in statistical parametric mapping (SPM; version 8; http://www.fil.ion.ucl.ac.uk/spm). GM and WM segmentations were combined to generate a robust brain mask, which was used to extract brains from skulls, which then entered the FreeSurfer pipeline. Subsequent steps involved Talairach transformation, GM/WM segmentation, and tessellation of the boundary between GM/WM to construct the WM surface including a correction of topological defects. After that, the pial surface was generated by inflation of the WM surface to the interface between GM and cerebrospinal fluid. The surface reconstruction generated a surface mesh model. CT was then defined as the shortest distance between a vertex on the reconstructed pial surface and the corresponding vertex on the WM surface and vice versa and then averaging both values.
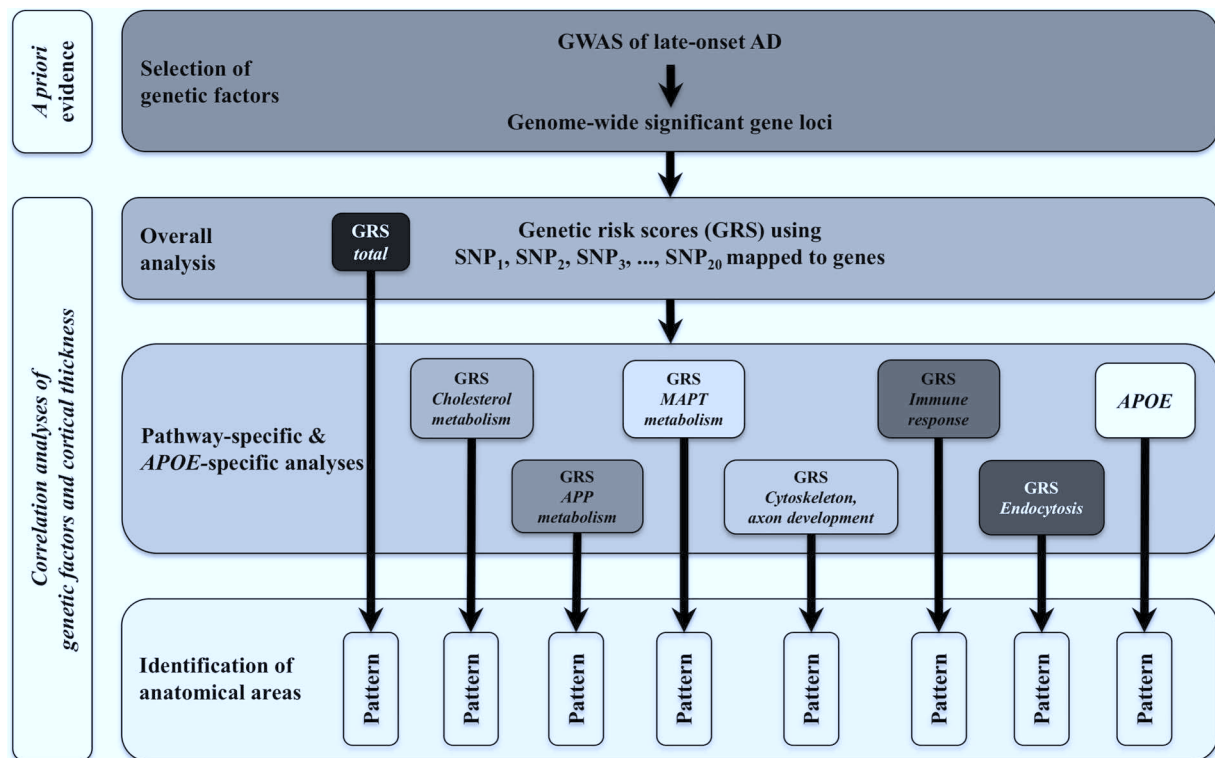
Figure 1. Overview of the study design.

The procedure resulted in ~150 000 measurements of CT per hemisphere, i.e., 300 000 vertices per whole brain. Finally, all CT maps were transformed onto the fsaverage brain template created in the Montreal Neurological Institute 305 space and smoothed using a Gaussian kernel of 10 mm.

Statistical Analysis

Computation of Genetic Risk Scores
The annotated SNP sets were used to generate GRS for each participant. GRS were calculated using weighted allelic scoring implemented in PLINK (version 1.9; https://www.cog-genomics.org/plink/1.9/score). In particular, effect alleles and sizes were defined according to Harold et al. (2009) and Lambert et al. (2013), i.e., the SNP effect (odds ratio, OR) corresponded to the log OR of the minor allele. A GRS value represented the mean of the summarized effects in a set of at least 2 SNPs. This procedure lead to 6 pathway-specific GRS (cholesterol metabolism, APP metabolism, MAPT metabolism, cytoskeleton/axon development, immune response, endocytosis), and a total GRS (total) that summarizes the effects across all pathways (overall analysis). Since epigenetics received support from only 1 SNP (rs1476679, ZCWPW1), an individual GRS for this pathway could not be calculated. However, the effect of rs1476679 was introduced to the GRS total. To follow-up the effect of *APOE*, *APOE*-adjusted pathway analyses and an *APOE*-specific single-gene analysis were performed. An overview of the study design is provided by Figure 1.

Correlation Analyses of GRS and CT
To assess CT differences in a population sample under the influence of a genetic burden for AD, any known factor that

possibly confound the statistical analysis of this relationship should be addressed by a correction. Age has a strong effect on brain structure and there are multiple studies that have systematically investigated this effect on imaging traits such as CT (Winkler et al. 2010). A very recent study of the large UK Biobank sample has provided convincing evidence for an influence of sex on CT, i.e., females show higher raw CT than males (Ritchie et al. 2018). Already patients with MCI, the prodromal stage of AD, show regional differences in CT compared to controls (Bakkour et al. 2013). Based on this knowledge, age, sex, and DemTect, were introduced as covariates to a general linear model (GLM) in all analyses. The GLM was implemented in FreeSurfer's QDEC interface (mri_glmfit). In the *APOE*-adjusted analyses, the GLM was additionally corrected for the *APOE*-$\varepsilon 4$ status (rs2075650). In each analysis, the lower and upper threshold of achievable significance levels (P-values) were set to $P = 0.05$ and $P = 1 \times 10^{-5}$. Finally, results were corrected for multiple testing using Monte Carlo simulation (mri_glmfit-sim tool with 10 000 iterations). Contiguous clusters of vertices indicating correlations between CT and GRS correlations were considered to be significant at a cluster-wise P-value (CWP) < 0.05. The pathway-specific GRS are based on SNP subsets from GRS total, i.e., each pathway analysis shows a full dependence from GRS total. Moreover, some pathways are partially dependent from each other since several of the investigated genes contribute to more than one pathway; all overlapping genes of the study are indicated as crossbars in Table 1. As a consequence, we have considered the overall analysis (GRS total) as the main analysis and each pathway analysis as a follow-up. A second correction for the number of tested pathways would require a complete independence of individual analyses. Since this requirement is not met
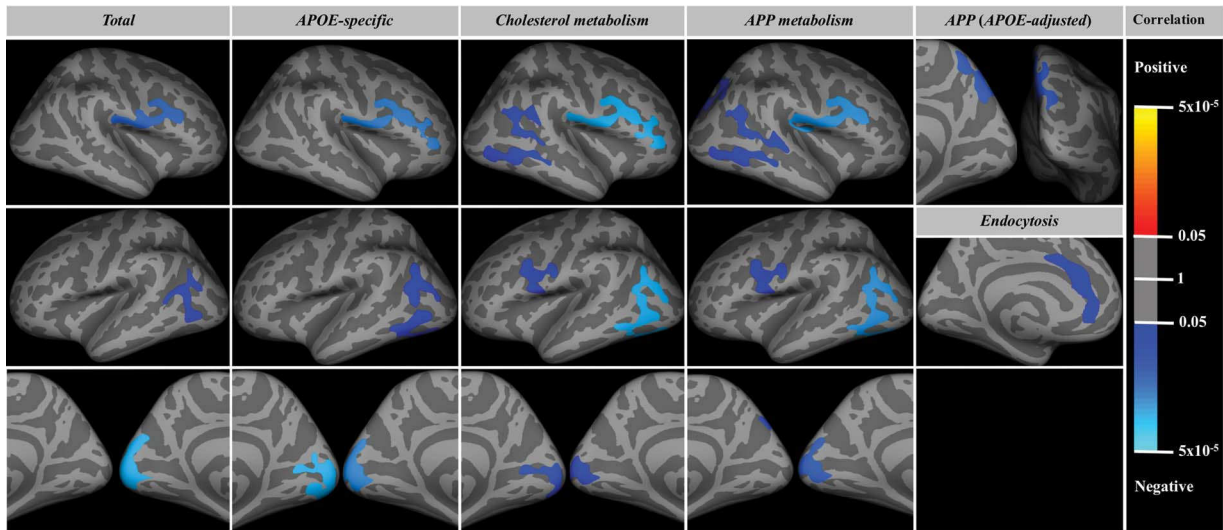
Figure 2. Patterns of cortical atrophy in older adults are influenced by genetic factors for late-onset AD. Dark gray regions represent sulci and light gray regions represent gyri on the inflated surface of the cortex. The blue colored clusters reflect significant negative correlations between the GRS and CT indicating atrophy in the GM (CWP < 0.05). Significant positive correlations (red clusters) were not observed. CWP values were encoded by a red-to-yellow color scale indicating a weak-to-strong positive correlation, while a dark blue-to-light blue color scale reflected a weak-to-strong negative correlation.

in our study design, CWP values were not additionally corrected.

Identification of Cortical Areas

To identify cortical areas, significant clusters were mapped to areas of the cytoarchitectonic JuBrain atlas (Zilles and Amunts 2010; http://jubrain.fz-juelich.de) using the SPM Anatomy Toolbox (version 2.2b by January 2016; Eickhoff et al. 2005). If a cluster did not overlap with a JuBrain area, because the cortical region has not been cytoarchitectonically mapped or the overlap between cluster and JuBrain area was too small, the localization of the cluster was described by a macroanatomical label. Identified JuBrain areas were denoted in accordance with the original publications.

Results

We identified significant clusters of vertices indicating negative correlations between CT and genetic factors for total, cholesterol metabolism, APP metabolism, APP metabolism adjusted for *APOE*, endocytosis, and *APOE*-specific (Fig. 2; Supplementary Fig. S2). The result of the overall analysis (total) was utilized as a basic reference to interpret CT changes of the pathway-specific and other follow-up analyses.

Overall Analysis

Three significant findings were generated by the GRS total: in the right hemisphere, a cluster (CWP = 1.0 × 10⁻³) encompassed the subcentral and ventral precentral gyrus and the caudally adjacent parietal operculum (area OP1; Eickhoff et al. 2006a; Eickhoff et al. 2006b) as well as the rostrally adjacent ventral precentral sulcus at the transition to caudal inferior frontal sulcus (IFS); in the left hemisphere, a cluster (CWP = 1.0 × 10⁻⁴) was located in the medial occipital cortex around the calcarine sulcus including primary, secondary, and dorsal extrastriate cortex (areas hOc1/V1, hOc2/V2, Amunts et al. 2000; hOc3d/V3d,

Kujovic et al. 2013), whereas another cluster (CWP = 3.4 × 10⁻²) spanned posterior parts of the middle temporal gyrus bordering the lateral occipital cortex (area hOc5, Malikovic et al. 2007) and reaching into the adjacent superior and inferior temporal sulci and the inferior temporal gyrus (ITG). In the GRS total-adjusted for *APOE* analysis, the pattern of 3 clusters did not appear. In the *APOE*-specific analysis, the pattern was found again, whereas the right frontal cluster extended more into rostral parts of the IFS, and the left temporal cluster extended more into the ITG; an additional cluster appeared in the right medial occipital cortex mirroring the respective left hemisphere occipital cluster.

Pathway-Specific Analyses

In the GRS analysis for cholesterol metabolism, the pattern of the overall analysis (total) re-appeared, but was amended by the contralateral counterparts of each cluster, giving rise to a symmetric, bilateral pattern. In the GRS analysis for APP metabolism, a similar bilateral pattern was found, except for the right occipital cluster. Instead, an additional cluster in the superior parietal cortex appeared (areas 7A, 7P; Scheperjans et al. 2008a; Scheperjans et al. 2008b), which was the only finding that survived the adjustment for *APOE* status (*APOE*-adjusted APP metabolism).

Patterns with unique clusters were generated in 2 analyses. In the GRS analysis for endocytosis, a cluster (CWP = 4.08 × 10⁻²) covered the left anterior cingulate cortex (ACC; areas 25a, 25p, s24a, s24b, s32, 33; Palomero-Gallagher et al. 2015) and the anterior midcingulate cortex (aMCC). Except for APP metabolism, other pathway-specific analyses were not significant after adjustment for the *APOE* status.

Discussion

In the present study, we investigated the cumulative effect of 20 LD-independent SNPs that had convincingly been reported to be associated with AD in large GWAS, on regional CT. We not only analyzed the effect of the combined effect of all 20 SNPs, but

also aimed to include a biologically meaningful sub-grouping of these SNPs. The rationale behind this concept is to group single GRS-SNPs that are falling into a common biological pathway and separate them from GRS-SNPs falling into other pathways because the biological mechanisms might act in different or even opposite directions. These considerations resulted in the analysis of GRS falling into 7 distinct biological pathways.

In a population sample of older adults, we found a common and pathway-specific patterns of cortical atrophy associated with genetic risk for late-onset AD. All findings showed that the higher the genetic burden, the stronger the GM deficit in the affected region. Most findings were influenced by the strong effect of the *APOE*.

Overall Analysis Reveals a Common Pattern of Cortical Thinning

The common pattern of cortical thinning that appeared consistently across the overall analysis and the pathway analyses for cholesterol metabolism and APP metabolism can be interpreted as a network of brain regions between the inferior frontal and adjacent precentral sulcus as well as the posterior temporal and medial occipital cortex. Although being highly focused to parts of these brain regions, our pattern showed similarity with atrophy patterns observed in patients with AD or MCI, the prodromal state of AD. Since results by Sabuncu et al. (2011), who has found patchy patterns across the entire cortex of patients with incipient AD compared to healthy controls, are elusive in this respect, other studies have provided more consistent observations. Cortical thinning in AD and MCI has particularly been found in the lateral prefrontal and premotor cortex, the posterior temporal as well as the adjacent anterior temporal and inferior parietal cortex (Dickerson et al. 2009; Lehman et al. 2011; Mak et al. 2015; Weston et al. 2016). Interestingly, the pattern of cortical thinning has been either more circumscribed or more extended in these studies, but some commonalities have been identified. The IFG was barely involved, instead, thinning extended from the IFS and adjacent precentral gyrus and spread into the dorsally adjacent lateral prefrontal cortex. While the extent in posterior brain regions was quite diverse, the posterior temporal cortex was always involved.

These observations are of particular interest with regard to our study since our sample was population-based and not selected for a low genetic burden of late-onset AD. We found cortical thinning only in the IFS and adjacent precentral sulcus among all frontal regions as well as in the posterior temporal cortex. It might thus be assumed that our common pattern reflects early cortical atrophy that is already detectable in healthy older adults. If these effects are specific to AD pathology or just observed as a result of the aging process has been controversially discussed (Bakkour et al. 2013; Fjell et al. 2014). In this respect, our result in the frontal lobe are of special interest as this largely resembles the AD-specific pattern of the IFS and the adjacent precentral sulcus that has reported to be distinct from aging-associated atrophy more localized to the IFG (Bakkour et al. 2013). In fact, the thinning in the inferior frontal cortex particularly reflected brain regions affected in incipient AD as compared to later stages of mild and moderate AD in which other brain regions showed predominant structural decline (Frisoni et al. 2009). Considering a continuum ranging from normal to diseased states of neurodegeneration (Liddell et al. 2007; Reinvang et al. 2013), our finding could represent a pattern of cortical thinning in normal aging that is driven by

genetic factors relevant for AD located at the disease end of the spectrum. Our results thus extend previous findings of MCI and AD to the normal end of the spectrum, arguing in favor for a continuum of changes in brain structure from healthy aging to neurodegeneration determined by orchestrated genetic risk for AD.

Another reason why such diverse atrophy patterns have been found in individuals carrying genetic risk factors for AD may be the heterogeneity of symptomatology at the beginning of AD. While typically dominated by episodic memory loss, late-onset AD might manifest with a diversity of symptoms affecting several cognitive domains, including dyspraxia, executive dysfunction, literacy, and language problems, as well as visuospatial and visuoperceptual dysfunctions (Galton et al. 2000; Dubois et al. 2010; McKhann et al. 2011; van der Flier et al. 2011; Crutch et al. 2012). This has been systematically assessed in a study with about 8000 patients (Barnes et al. 2015), showing a considerable heterogeneity in the first cognitive or behavioral symptoms associated with AD, with cognitive symptoms (language, problem solving, and visuospatial dysfunction) yielding larger ORs. However, it has not been investigated if these dysfunctions are accompanied with deficits in the underlying brain structure. Hence, our results in the occipital cortex are highly interesting since 60% of dementias with visual dysfunction are attributable to AD (Armstrong and Kergoat 2015). In late MCI, first atrophy rates in the visual system can be detected at the lingual gyrus and lateral occipital cortex (McDonald et al. 2009). In incipient AD, atrophy spreads further at the medial occipital cortex (Frisoni et al. 2009), especially in the cuneus (McDonald et al. 2009). The severe atrophy in the visual system has been found at the occipital pole in moderate AD (Frisoni et al. 2009).

It is noteworthy that the common pattern was mainly driven by the *APOE-ε4* allele since the *APOE*-specific analysis yielded almost the same pattern as found for the overall analysis. The additional bilaterality of the medial occipital cluster might be a matter of counteracting effects from genetic variants in the GRS total, which are absent in the single-locus analysis of *APOE*, thus potentially allowing for a more expanded pattern. To reveal such counter-acting effects from individual and/or subgroups of SNPs, we prepared uncorrected CT maps where the *APOE* effects and subtle effects from other SNPs were clearly visible (Supplementary Fig. S3). Using a comparable GRS approach to investigate effects of biological pathways, Darst et al. (2016) have found *APOE* as being the driving factor for cognition function and beta-amyloid deposition in older individuals with increased risk for AD. Moreover, our results showed that a statistical adjustment against the *APOE* effect in the overall and pathway-specific analyses resulted in negative findings, apart from a thinning in the posterior parietal cortex (precuneus) in the GRS analysis for APP metabolism. A plausible explanation for these observations is that the *ε*4 allele, as tagged by SNP rs2075650, has a comparably strong OR of 2.53. We assume that the remaining mix of effects (ORs between 1.22 and 0.77) was not strong enough to withstand correction for multiple comparisons. Hence, our results provide further evidence for a key role of *APOE* in AD-associated alterations and pathology. To further disentangle these aspects, future analyses with larger and longitudinal data are warranted.

Pathway-Specific Variations of the Common Pattern

The stratification of the overall effects (GRS total) into pathway-specific effects facilitated the discovery of 2 variations of the

common pattern. The common pattern was generally found symmetrically in both hemispheres (Lehmann et al. 2011; Mak et al. 2015), but partially also slightly right-lateralized in AD patients (Dickerson et al. 2009). While methodological reasons cannot be excluded, such as threshold or power issues, a biological underpinning might also be plausible. Our results might add up to this discussion from a genetic perspective. While the common pattern observed in the overall and *APOE*-specific analyses revealed an inconclusive picture in terms of lateralization, the APP metabolism and cholesterol metabolism analyses led to symmetrical, bilateral patterns in both inferior frontal and posterior temporal cortex. With the common pattern being mainly driven by *APOE*, it might be the case that other genetic variants could have partially counteracted the detrimental *APOE* effect, leading to non-significant thinning effects in one side of the brain, as discussed above. Both cholesterol metabolism and APP metabolism, contrarily, contain only a few variants in addition to *APOE-e4*. This might have led to more regions where thinning becomes significant, e.g., due to variation in *ABCA7* and *INPP5D* which might have enhanced the *APOE* effect.

A unique pattern was identified in the GRS analysis for endocytosis, where a cortical thinning in the left ACC and aMCC was found, while cortical regions occurring within other atrophy patterns were spared. While a tendency towards such a pattern could be recognized in AD patients compared to healthy controls (Mak et al. 2015), the same study revealed a much more prominent association within this brain region: AD patients with pronounced deficits in visuospatial memory had predominant cortical atrophy particularly in the left ACC and adjacent aMCC. Involved in a variety of functions and emotional regulation, the ACC/aMCC region is also involved in cognitive and executive control, particularly for tasks with high working memory load (Paus et al. 1998; Umemoto and Holroyd 2016), which appears to be particularly impaired in AD patients and associated with respective cortical atrophy in this brain region (Mak et al. 2015).

The remaining pathway analyses (MAPT metabolism, cytoskeleton, immune response) did not reveal any significant CT change. Reasons may be small sample size, stringent control for multiple comparison, counteracting genetic effects, and biological cause. Since MAPT metabolism was the only pathway of tau pathology in the present study it might be an interesting gene set for more detailed assessment in future studies.

Strengths, Limitations, and Concluding Remarks

Given that CT is sensitive for GM changes and the investigated loci most likely contribute to AD susceptibility, we quantified the effects of the underlying common genetic variation on CT using a targeted GRS. This kind of GRS that solely based on a small set of highly selected SNPs has been proven successful in several studies of cognition and brain structure (Sabuncu et al. 2012; Verhaaren et al. 2013; Darst et al. 2016; Habes et al. 2016; Harrison et al. 2016; Louwersheimer et al. 2016). Of these, only Sabuncu et al. (2012) have focused on aging, AD risk, and CT in selected, clinically normal individuals. Our study sample, however, was drawn from a population-based cohort and no exclusion criteria, except MRI safety reasons, were applied. Therefore, our results reflect an association between genetic risk for late-onset AD and CT across a wide spectrum of normally aging older individuals. We did not replicate the findings in an independent sample. However, our sample was 5 times larger than that of the Sabuncu

et al. (2012) study. Moreover, we used a very stringent statistical threshold for selection of AD-associated SNPs (genome-wide significance in GWAS of AD) to allow in-depth investigation of literature-supported biological pathways underlying changes of cortical structure in normal aging. We did not investigate the relation between the total and pathway-specific GRS with cerebrospinal fluid biomarkers for beta-amyloid peptide and tau protein, as no such data were available for our sample (1000BRAINS). Since previous studies have sought for association between such biomarkers and brain structure and function (e.g., Sabuncu et al. 2011; Sabuncu et al. 2012; Darst et al. 2016), this will be an interesting aspect for follow-up studies using suitable study samples.

Based on the outcome of our study, we conclude that in later decades of life, susceptibility for AD may explain a fraction of the inter-individual variability of CT suggesting a partially overlapping genetic basis for structural brain changes within the spectrum from normal aging to neurodegenerative disease. Due to the complexity of biological processes underlying the association between *APOE* and late-onset AD as well as *APOE* and non-pathological aging (Reinvang et al. 2013), longitudinal and larger studies are warranted to further dissect the association between AD and cortical thinning in older individuals.

Supplementary Material

Supplementary material is available at *Cerebral Cortex* online.

Funding

Notes

References

Allen M, Kachadoorian M, Carrasquillo MM, Karhade A, Manly L, Burgess JD, Wang C, Serie D, Wang X, Siuda J *et al*. 2015. Late-onset Alzheimer disease risk variants mark brain regulatory loci. *Neurol Genet*. 1:e15.

Amunts K, Malikovic A, Mohlberg H, Schormann T, Zilles K. 2000. Brodmann's areas 17 and 18 brought into stereotaxic space—where and how variable? *Neuroimage*. 11:66–84.

Armstrong R, Kergoat H. 2015. Oculo-visual changes and clinical considerations affecting older patients with dementia. *Ophthalmic Physiol Opt*. 35:352–376.

Ashburner J, Friston KJ. 2005. Unified segmentation. *Neuroimage*. 26:839–851.

Bakkour A, Morris JC, Wolk DA, Dickerson BC. 2013. The effects of aging and Alzheimer's disease on cerebral cortical anatomy: specificity and differential relationships with cognition. *Neuroimage*. 76:332–344.

Barnes J, Dickerson BC, Frost C, Jiskoot LC, Wolk D, van der Flier WM. 2015. Alzheimer's disease first symptoms are age dependent: evidence from the NACC dataset. *Alzheimers Dement.* 11:1349–1357.

Caspers S, Moebus S, Lux S, Pundt N, Schütz H, Mühleisen TW, Gras V, Eickhoff SB, Romanzetti S, Stöcker T *et al.* 2014. Studying variability in human brain aging in a population-based German cohort—rationale and design of 1000BRAINS. *Front Aging Neurosci.* 6:1–14.

Chapuis J, Hansmannel F, Gistelinck M, Mounier A, Van Cauwenberghe C, Kolen KV, Geller F, Sottejeau D, Harold D, Dourlen P *et al.* 2013. Increased expression of BIN1 mediates Alzheimer genetic risk by modulating tau pathology. *Mol Psychiatry.* 18:1225–1234.

Chauhan G, Adams HHH, Bis JC, Weinstein G, Yu L, Töglhofer AM, Smith AV, van der Lee SJ, Gottesman RF, Thomson R *et al.* 2015. Association of Alzheimer's disease GWAS loci with MRI markers of brain aging. *Neurobiol Aging.* 36:1765.e7–1765.e16.

Crutch SJ, Lehmann M, Schott JM, Rabinovici GD, Rossor MN, Fox NC. 2012. Posterior cortical atrophy. *Lancet Neurol.* 11:170–178.

Dale AM, Fischl B, Sereno MI. 1999. Cortical surface-based analysis I. Segmentation and surface reconstruction. *Neuroimage.* 9:179–194.

Darst BF, Koscik RL, Racine AM, Oh JM, Krause RA, Carlsson CM, Zetterberg H, Blennow K, Christian BT, Bendlin BB *et al.* 2016. Pathway-specific polygenic risk scores as predictors of amyloid-β deposition and cognitive function in a sample at increased risk for Alzheimer's disease. *J Alzheimers Dis.* 55:473–484.

Dickerson BC, Bakkour A, Salat DH, Feczko E, Pacheco J, Greve DN, Grodstein F, Wright CI, Blacker D, Rosas HD *et al.* 2009. The cortical signature of Alzheimer's disease: regionally specific cortical thinning relates to symptom severity in very mild to mild AD dementia and is detectable in asymptomatic amyloid-positive individuals. *Cereb Cortex.* 19:497–510.

Dubois B, Feldman HH, Jacova C, Cummings JL, DeKosky ST, Barberger-Gateau P, Delacourte A, Frisoni G, Fox NC, Galasko D *et al.* 2010. Revising the definition of Alzheimer's disease: a new lexicon. *Lancet Neurol.* 9:1118–1127.

Eickhoff SB, Stephan KE, Mohlberg H, Grefkes C, Fink GR, Amunts K, Zilles K. 2005. A new SPM toolbox for combining probabilistic cytoarchitectonic maps and functional imaging data. *Neuroimage.* 25:1325–1335.

Eickhoff SB, Schleicher A, Zilles K, Amunts K. 2006a. The human parietal operculum: I. Cytoarchitectonic mapping of subdivisions. *Cereb Cortex.* 16:254–267.

Eickhoff SB, Amunts K, Mohlberg H, Zilles K. 2006b. The human parietal operculum: II. Stereotaxic maps and correlation with functional imaging results. *Cereb Cortex.* 16:268–279.

Fischl B, Sereno MI, Dale AM. 1999. Cortical surface-based analysis II: Inflation, flattening, and a surface-based coordinate system. *Neuroimage.* 9:195–207.

Fischl B, Dale AM. 2000. Measuring the thickness of the human cerebral cortex from magnetic resonance images. *Proc Natl Acad Sci U S A.* 97:11050–11055.

Fjell AM, McEvoy L, Holland D, Dale AM, Wallhovd KB, Alzheimer's Disease Neuroimaging Initiative. 2014. What is normal in normal aging? Effects of aging, amyloid and Alzheimer's disease on the cerebral cortex and the hippocampus. *Prog Neurobiol.* 117:20–40.

Foley SF, Tansey KE, Caseras X, Lancaster T, Bracht T, Parker G, Hall J, Williams J, Linden DEJ. 2017. Multimodal brain imaging reveals structural differences in Alzheimer's disease polygenic risk carriers: a study in healthy young adults. *Biol Psychiatry.* 81:154–161.

Frisoni GB, Prestia A, Rasser PE, Bonetti M, Thompson PM. 2009. In vivo mapping of incremental cortical atrophy from incipient to overt Alzheimer's disease. *J Neurol.* 256:916–924.

Galton CJ, Patterson K, Xuereb JH, Hodges JR. 2000. Atypical and typical presentations of Alzheimer's disease: a clinical, neuropsychological, neuroimaging and pathological study of 13 cases. *Brain.* 123:484–498.

Goh JO, Park DC. 2009. Neuroplasticity and cognitive aging: the scaffolding theory of aging and cognition. *Restor Neurol Neurosci.* 27:391–403.

Guerreiro R, Brás J, Hardy J. 2013. SnapShot: genetics of Alzheimer's disease. *Cell.* 155:968.

Habes M, Janowitz D, Erus G, Toledo JB, Resnick SM, Doshi J, Van der Auwera S, Wittfeld K, Hegenscheid K, Hoston N *et al.* 2016. Advanced brain aging: relationship with epidemiologic and genetic risk factors, and overlap with Alzheimer disease atrophy patterns. *Transl Psychiatry.* 6:e775.

Harold D, Abraham R, Hollingworth P, Sims R, Gerrish A, Hamshere ML, Pahwa JS, Moskvina V, Dowzell K, Williams A *et al.* 2009. Genome-wide association study identifies variants at CLU and PICALM associated with Alzheimer's disease. *Nat Genet.* 41:1088–1093.

Harris SE, Davies G, Luciano M, Payton A, Fox HC, Haggarty P, Ollier W, Horan M, Porteous DJ, the Genetic and Environmental Risk for Alzheimer's disease Consortium *et al.* 2014. Polygenic risk for Alzheimer's disease is not associated with cognitive ability or cognitive aging in non-demented older people. *J Alzheimers Dis.* 39:565–574.

Harrison TM, Mahmood Z, Lau EP, Karacozoff AM, Burggren AC, Small GW, Bookheimer SY. 2016. An Alzheimer's disease genetic risk score predicts longitudinal thinning of hippocampal complex subregions in healthy older adults. *eNeuro.* 3: ENEURO 0098-16:2016.

Hwang J, Kim CM, Jeon S, Lee JM, Hong YJ, Roh JH, Lee JH, Koh JH, Na GL, Alzheimer's Disease Neuroimaging Initiative. 2016. Prediction of Alzheimer's disease pathophysiology based on cortical thickness patterns. *Alzheimers Dement (Amst).* 2:58–67.

Kalbe E, Kessler J, Calabrese P, Smith R, Passmore AP, Brand M, Bullock R. 2004. DemTect: a new, sensitive cognitive screening test to support the diagnosis of mild cognitive impairment and early dementia. *Int J Geriatr Psychiatry.* 19:136–143.

Karch CM, Goate AM. 2015. Alzheimer's disease risk genes and mechanisms of disease pathogenesis. *Biol Psychiatry.* 77:43–51.

Karch CM, Ezerskiy LA, Bertelsen S, Alzheimer's Disease Genetics Consortium, Goate AM. 2016. Alzheimer's disease risk polymorphisms regulate gene expression in the ZCWPW1 and the CELF1 loci. *PloS One.* 11:e0148717.

Karlawish J, Jack CR, Rocca WA, Snyder HM, Carillo MC. 2017. Alzheimer's disease: the next frontier—special report 2017. *Alzheimers Dement.* 13:374–380.

Kujovic M, Zilles K, Malikovic A, Schleicher A, Mohlberg H, Rottschy C, Eickhoff SB, Amunts K. 2013. Cytoarchitectonic mapping of the human dorsal extrastriate cortex. *Brain Struct Funct.* 218:157–172.

Lambert JC, Ibrahim-Verbaas CA, Harold D, Naj AC, Sims R, Bellenguez C, Jun G, DeStefano AL, Bis JC, Beecham GW *et al.* 2013. Meta-analysis of 74,046 individuals identifies 11 new susceptibility loci for Alzheimer's disease. *Nat Genet.* 45:1452–1458.

Lehmann M, Crutch SJ, Ridgway GR, Ridha BH, Barnes J, Warrington EK, Rossor MN, Fox NC. 2011. Cortical thickness and voxel-based morphometry in posterior cortical atrophy and typical Alzheimer's disease. *Neurobiol Aging*. 32:1466–1476.

Liddell BJ, Paul RH, Arns M, Gordon N, Kukla M, Rowe D, Cooper N, Moyle J, Williams LM. 2007. Rates of decline distinguish Alzheimer's disease and mild cognitive impairment relative to normal aging: integrating cognition and brain function. *J Integr Neurosci*. 6:141–174.

Louwersheimer E, Wolfsgruber S, Espinosa A, Lacour A, Heilmann-Heimbach S, Alegret M, Hernández I, Rosende-Roca M, Tárraga L, Boada M et al. 2016. Alzheimer's disease risk variants modulate endophenotypes in mild cognitive impairment. *Alzheimers Dement*. 12:872–881.

Lupton MK, Strike L, Hansell NK, Wen W, Mather KA, Armstrong NJ, Thalamuthu A, McMahon KL, de Zubicaray GI, Assareh AA et al. 2016. The effect of increased genetic risk for Alzheimer's disease on hippocampal and amygdala volume. *Neurobiol Aging*. 40:68–77.

Mak E, Su L, Williams GB, Watson R, Firbank MJ, Blamire AM, O'Brien JT. 2015. Progressive cortical thinning and subcortical atrophy in dementia with Lewy bodies and Alzheimer's disease. *Neurobiol Aging*. 36:1743–1750.

Malikovic A, Amunts K, Schleicher A. 2007. Cytoarchitectonic analysis of the human extrastriate cortex in the region of V5/MT+: a probabilistic, stereotaxic map of area hOc5. *Cereb Cortex*. 17:562–574.

Martiskainen H, Helisalmi S, Viswanathan J, Kurki M, Hall A, Herukka SK, Sarajärvi T, Natunen T, Kurkinen KMA, Huvinen J et al. 2015. Effects of Alzheimer's disease-associated risk loci on cerebrospinal fluid biomarkers and disease progression: a polygenic risk score approach. *J Alzheimers Dis*. 43:565–573.

McDonald CR, McEvoy LK, Gharapetian L, Fennema-Notestine C, Hagler DJ, Holland D, Koyama A, Brewer JB, Dale AM. 2009. Regional rates of neocortical atrophy from normal aging to early Alzheimer disease. *Neurology*. 73:457–465.

McKhann GM, Knopman DS, Chertkow H, Hyman BT, Jack CR, Kawas CH, Klunk WE, Koroshetz WJ, Manly JJ, Mayeux R et al. 2011. The diagnosis of dementia due to Alzheimer's disease: recommendations from the National Institute on Aging-Alzheimer's association workgroups on diagnostic guidelines for Alzheimer's disease. *Alzheimers Dement*. 7:263–269.

Mormino EC, Sperling RA, Holmes AJ, Buckner RL, De Jager PL, Smoller JW, Sabuncu MR. 2016. Polygenic risk of Alzheimer disease is associated with early- and late-life processes. *Neurology*. 87:481–488.

Palomero-Gallagher N, Eickhoff SB, Hoffstaedter F, Schleicher A, Mohlberg H, Vogt BA, Amunts K, Zilles K. 2015. Functional organization of human subgenual cortical areas: relationship between architectonical segregation and connectional heterogeneity. *Neuroimage*. 115:177–190.

Park DC, Reuter-Lorenz P. 2009. The adaptive brain: aging and neurocognitive scaffolding. *Annu Rev Psychol*. 60:173–196.

Paus T, Koski L, Caramanos Z, Westbury C. 1998. Regional differences in the effects of task difficulty and motor output on blood flow response in the human anterior cingulate cortex: a review of 107 PET activation studies. *Neuroreport*. 9:R37–R47.

Pini L, Pievani M, Bocchetta M, Altomore F, Bosco P, Cavedo E, Galluzzi S, Marizzoni M, Frisoni GB. 2016. Brain atrophy in Alzheimer's disease and aging. *Ageing Res Rev*. 30:25–48.

R Development Core Team. 2010. R: a language and environment for statistical computing [Computer programme]. URL http://www.R-project.org/.

Reinvang I, Espeseth T, Westlye LT. 2013. APOE-related biomarker profiles in non-pathological aging and early phases of Alzheimer's disease. *Neurosci Biobehav Rev*. 37: 1322–1335.

Reuter-Lorenz PA, Lustig C. 2005. Brain aging: reorganizing discoveries about the aging mind. *Curr Opin Neurobiol*. 15:245–251.

Reuter-Lorenz PA, Park DC. 2014. How does it STAC up? Revisiting the scaffolding theory of aging and cognition. *Neuropsychol Rev*. 24:355–370.

Ritchie SJ, Cox SR, Shen X, Lombardo MV, Reus LM, Alloza C, Harris MA, Alderson HL, Hunter S, Neilson E et al. 2018. Sex differences in the adult human brain: evidence from 5216 UK biobank participants. *Cerebral Cortex*. 28(8):2959–2975.

Rosenthal SL, Kamboh MI. 2014. Late-onset Alzheimer's disease genes and the potentially implicated pathways. *Curr Genet Med Rep*. 2:85–101.

Sabuncu MR, Desikan RS, Sepulcre J, Yeo BTT, Liu H, Schmansky NJ, Reuter M, Weiner MW, Buckner RL, Sperling RA et al. 2011. The dynamics of cortical and hippocampal atrophy in Alzheimer disease. *Arch Neurol*. 68:1040–1048.

Sabuncu MR, Buckner RL, Smoller JW, Lee PH, Fischl B, Sperling RA. 2012. The association between a polygenic Alzheimer score and cortical thickness in clinically normal subjects. *Cereb Cortex*. 22:2653–2661.

Saunders AM, Roses AD, Pericak-Vance MA, Dole KC, Strittmatter WJ, Schmechel DE, Szymanski MH, McCown N, Manwaring MG, Schmader K et al. 1993. Apolipoprotein E epsilon 4 allele distributions in late-onset Alzheimer's disease and in other amyloid-forming diseases. *Lancet*. 342:710–711.

Scheperjans F, Hermann K, Eickhoff SB, Amunts K, Schleicher A, Zilles K. 2008a. Observer-independent cytoarchitectonic mapping of the human superior parietal cortex. *Cereb Cortex*. 18:846–867.

Scheperjans F, Eickhoff SB, Hömke L, Mohlberg H, Hermann K, Amunts K, Zilles K. 2008b. Probabilistic maps, morphometry, and variability of cytoarchitectonic areas in the human superior parietal cortex. *Cereb Cortex*. 18:2141–2157.

Schmermund A, Möhlenkamp S, Stang A, Grönemeyer D, Seibel R, Hirche H, Mann K, Siffert W, Lauterbach K, Siegrist J et al. 2002. Assessment of clinically silent atherosclerotic disease and established and novel risk factors for predicting myocardial infarction and cardiac death in healthy middle-aged subjects: rationale and design of the Heinz Nixdorf RECALL study. Risk factors, evaluation of coronary calcium and lifestyle. *Am Heart J*. 144:212–218.

Sims R, Williams J. 2016. Defining the genetic architecture of Alzheimer's disease: where next. *Neurodegener Dis*. 16:6–11.

Strittmatter WJ, Saunders AM, Schmechel D, Pericak-Vance M, Enghild J, Salvesen GS, Roses AD. 1993. Apolipoprotein E: high-avidity binding to beta-amyloid and increased frequency of type 4 allele in late-onset familial Alzheimer disease. *Proc Natl Acad Sci U S A*. 90:1977–1981.

Umemoto A, Holroyd CB. 2016. Exploring individual differences in task switching. Persistence and other personality traits related to anterior cingulate cortex function. *Prog Brain Res*. 229:189–212.

Van Cauwenberghe C, Van Broeckhoven C, Sleegers K. 2016. The genetic landscape of Alzheimer disease: clinical implications and perspectives. *Genet Med*. 18:421–430.

Van der Flier WM, Pijnenburg YA, Fox NC, Scheltens P. 2011. Early-onset versus late-onset Alzheimer's disease: the case of the missing APOE ε4 allele. *Lancet Neurol*. 10:280–288.

Verhaaren BF, Vernooij MW, Koudstaal PJ, Uitterlinden AG, van Duijn CM, Hofman A, Breteler MMB, Ikram MA. 2013. Alzheimer's disease genes and cognition in the nondemented general population. *Biol Psychiatry*. 73:429–434.

Weston PS, Nicholas JM, Lehmann M, Ryan NS, Liang Y, Macpherson K, Modat M, Rossor MN, Schott JM, Ourselin S *et al.* 2016. Presymptomatic cortical thinning in familial Alzheimer disease—a longitudinal MRI study. *Neurology*. 87:2050–2057.

Winkler AM, Kochunov P, Blangero J, Almasy L, Zilles K, Fox PT, Duggirala R, Glahn DC. 2010. Cortical thickness or grey matter volume? The importance of selecting the phenotype for imaging genetics studies. *Neuroimage*. 53:1135–1146.

Zilles K, Amunts K. 2010. Centenary of Brodmann's map—conception and fate. *Nat Rev Neurosci*. 11:139–145.